Science Translational Medicine
AAAS

www.sciencetranslationalmedicine.org/cgi/content/full/10/433/eaao5945/DC1

Supplementary Materials for

Vaccine waning and mumps re-emergence in the United States

Joseph A. Lewnard* and Yonatan H. Grad*

*Corresponding author. Email: jlewnard@hsph.harvard.edu (J.A.L.); ygrad@hsph.harvard.edu (Y.H.G.)

Published 21 March 2018, *Sci. Transl. Med.* **10**, eaao5945 (2018)
DOI: 10.1126/scitranslmed.aao5945

This PDF file includes:

Materials and Methods
Fig. S1. Fitted endemic transmission dynamics before vaccine rollout.
Fig. S2. Reductions in mumps notifications correspond with increases in vaccine coverage and a declining basic reproductive number.
Fig. S3. Birth cohorts accounting for reported cases over time.
Fig. S4. Changes in estimates of the susceptible population under scenarios of declining reporting.
Fig. S5. Changes in estimates of R_0 over time under scenarios of declining reporting.
Fig. S6. Aggregated age-specific notification rates.
Fig. S7. Estimates of population susceptibility and $R_0(t)$ under an assumption of time-invariant protection.
Table S1. Studies included in meta-analysis assessing vaccine waning.
Table S2. Model parameter definitions and values.
References (*46–48*, *50*, *55–81*)

Materials and Methods

Meta-analytic estimation of vaccine waning rates

Literature search

We performed a systematic literature search to identify studies from which we could infer variation in vaccine effectiveness. We searched the Boolean phrase

mumps AND vaccin* AND ((second* AND fail*) OR wan*)

in PubMed (obtaining 77 results) and Google Scholar (considering the first 300 results). We also aggregated all references listed in three recent articles *(9, 12, 14)* reviewing studies of mumps vaccine performance (totaling 234 results), and all citations of these three articles in Google Scholar (totaling 370 results as of 6 June 2017). We similarly performed forward- and back citation tracking of included studies. We included articles:

1. written in English;
2. presenting results of prospective or retrospective cohort studies of mumps vaccination and disease incidence, and thereby enabling calculation of the relative risk of laboratory-confirmed clinical mumps according to vaccination status;
3. clearly indicating the time elapsed between receipt of the last vaccine dose and onset of exposure to mumps transmission; and
4. (if individuals in the study were born within five years after the introduction of routine mumps vaccination): excluding individuals with serologic or clinical history of mumps infection, thus preventing misclassification bias that could otherwise be confused for evidence of vaccine waning *(46)*. We assumed low risk of previous mumps infection for individuals born more than five years after implementation of routine vaccination.

Two studies *(47, 48)* which met the conditions listed above were excluded from the analysis because they lacked an unvaccinated reference population, preventing the estimation of effect sizes. The included studies are listed in **table S1**.

We obtained the number of mumps cases reported among total vaccinated and unvaccinated study populations together with vaccination status and time from vaccination to exposure. When possible, we extracted subsamples from individual studies wherein subjects differed in time since vaccination.

Testing for differences in protection with time since vaccination

We fitted an inverse variance-weighted model of log-transformed relative risk estimates against time since vaccination, allowing for fixed study-level effects based on a comparison of the Bayesian Information Criterion from fixed- and random-effects models (BIC_{FE}=69.6, BIC_{RE}=73.6). By this same measure, the model including time since receipt of the last dose provided a better fit to data than a null model with study-level intercepts alone (BIC_{null}=103.1). We measured the proportion of residual variance from the null model (M^0) explained by the model including time since last dose (M^*) as the reduction in weighted squared errors:

$$1 - \frac{\sum_i w_i \left(Y_i - \hat{Y}_i^*\right)^2}{\sum_i w_i \left(Y_i - \hat{Y}_i^0\right)^2} = 0.664.$$

Weights w_i were proportional to the inverse of the variance of estimates Y_i from original studies. Calculated from the pseudo-R^2 value, the model including time since last dose and study-level intercepts explained 88.9% of variation in previous estimates of effectiveness.

We next tested whether waning rates differed for children who had received one or two doses of vaccine. Excluding one study which presented aggregated data from 1-dose and 2-dose recipients *(51)*, we identified no improvement in model fit when allowing for differential rates of loss of protection among 1-dose and 2-dose recipients ($BIC_{\text{Any-dose}}$=56.1, $BIC_{\text{Dose-specific}}$=58.3).

Estimating rates of waning of vaccine-derived protection

Our analysis of aggregated data from studies did not allow us to infer the distribution of waning rates across individuals. As a result, assuming exponentially-distributed time to loss of protection provided the most parsimonious basis for predicting for the proportion of vaccinated individuals who, conditioned upon initial vaccine "take", would retain protection at a given time. We further assumed our estimate of vaccine effectiveness at 6 months from the above regression model approximated the proportion of doses initially conferring protection (ν), as 6 months was the shortest average duration of follow-up from time of vaccination among included studies (**table S1**). Our estimate of vaccine effectiveness at this time point was 96.4% (94.0-97.8%).

We fitted an exponential waning rate ω_V by minimizing the sum of squared errors between:

1. the proportion of individuals initially protected by the vaccine who retain protection under exponentially-distributed durations of protection, $\exp(-\omega_V t)/\nu$, where t indicates years since receipt of the last dose (t>0.5), and

2. estimates of the ratio of vaccine effectiveness at time t to time t=0.5 under the meta-regression model:

$$\underset{\omega_V}{\operatorname{argmin}} \left\{ \sum_t \left(\frac{\exp[-\omega_V (t - 0.5)]}{\nu} - \frac{\hat{Y}_t^*}{\hat{Y}_{t=0.5}^*} \right)^2 \right\}$$

for t={0.5, 0.51, 0.52, …, 18.5}, corresponding to the range of observations included in the original estimates (**table S1**). To propagate uncertainty from the initial regression estimates, we constructed the distribution of ω_V by fitting against independent samples of $\{\nu, \hat{\boldsymbol{Y}}^*\}$ obtained from the multivariate-normal distribution of regression parameters.

Inferring transmission dynamics in the pre-vaccination era

Model of mumps transmission

We modeled steady-state transmission dynamics of mumps in the US prior to vaccine introduction (1967) to estimate starting-time, age-specific prevalence of susceptibility and naturally acquired immunity, and to infer reporting rates. Our model accounted for transitions among susceptible (S), exposed (E), infectious (I), and recovered-immune (R) classes, $N = S+E+I+R$, assuming infectiousness begins, on average, σ^{-1}=17 days after exposure and lasts, on average, γ^{-1}=5 days *(55)*. We partitioned the population across age classes (0-11m, 1-4y, 5-9y, 10-14y, 15-19y, 20-24y, 25-29y, 30-39y, 40-64y, ≥65y) corresponding to the ranges for reporting of aggregated case data *(56)*, and defining the rate of aging from the i^{th} class as $\alpha(i)$. For tractability we assumed a stable population, so that births into the youngest class were equal to deaths from the oldest class, i.e., $\mu(1) = \alpha(10)N(10)$. The force of infection $\lambda(i)$ is the rate of infection in the susceptible class. Taken together,

$$\dot{S}(i) = \mu(i) - [\lambda(i) + \alpha(i)]S(i) + \alpha(i-1)S(i-1),$$
$$\dot{E}(i) = \lambda(i)S(i) - [\sigma + \alpha(i)]E(i) + \alpha(i-1)E(i-1),$$
$$\dot{I}(i) = \sigma E(i) - [\gamma + \alpha(i)]I(i) + \alpha(i-1)I(i-1),$$
$$\dot{R}(i) = \gamma I(i) - \alpha(i)R(i) + \alpha(i-1)R(i-1),$$
$$\lambda(i) = \beta(i)\sum_{j=1}^{10} C_{(S)}(i,j)\frac{I(j)}{N(j)}.$$

The force of infection $\lambda(i)$ arises from age-structured social mixing in the context of differential age-specific prevalence of infection. We rescaled matrix elements $C_{(S)}(i, j)$ from diary data of daily, age-specific respiratory contacts from the UK *(57)* to accommodate the age distribution of the population, as modeled, with equal birth and death rates, and made elements symmetric

$$C_{(S)}(i,j) = \frac{C_{Reported}(i,j) + C_{Reported}(j,i)}{2}$$

to correct for biased responses. We fitted $\beta(i)$ for each age group to allow flexibility, for instance due to differences from contact patterns reported by survey participants, differences across ages in risk for infection given exposure (as may arise since young children are more likely to put their hands or objects in their mouths), and differential susceptibility across ages due to factors other than infection-derived or vaccine-derived immunity (for instance, maternal antibody-mediated protection in the first year of life).

Model parameters are listed with sources and definitions in **table S2**. Replication code including parameter distributions and estimates of time-varying parameters is available at https://github.com/joelewnard/mumps.

Parameter estimation

We estimated parameters allowing the model to recapitulate reported age-specific incidence rates over the years 1960-1964 in the US *(58)*. Simulating 150y of transmission to achieve steady-state conditions, and recording the force of infection and susceptible population at equilibrium, we used the Nelder Mead algorithm to perform weighted least-squares estimation

$$\underset{\{\rho,\boldsymbol{\beta}\}}{\operatorname{argmin}} \left(\sum_{i=1}^{10} w(i) \left(\Lambda(i) - \rho\lambda(i) \, \frac{S(i)}{N(i)} \right)^2 \right)$$

mapping reported age-specific incidence rates $\Lambda(i)$ to model-predicted rates of infection, scaled by the proportion of infections reported (ρ). So that absolute discrepancies were penalized relative to the true value, we defined weights $w(i)=[1+\Lambda(i)]^{-1}$.

Our model-based estimate that ρ=3.7% closely corroborates the estimate of 4.0% (95%CI: 1.3–8.0%) obtained from comparisons of surveillance data against community serosurveys *(59)*. The basic reproductive number (R_0=4.79) during the pre-vaccination era is the maximum eigenvalue of the matrix composed of elements

$$\frac{\beta(i)C_{(S)}(i,j)N(i)}{\gamma N(j)}.$$

Providing a good fit to data, the model predicted 59% of individuals would acquire infection between the ages of 5 and 9, and that 89% would be infected by age 20 (**fig. S1**).

We also used the model to assess whether naturally-acquired immunity was likely to wane, assuming individuals exited the *R* class and re-entered the *S* class at a rate ω_N. Our estimate that such waning would occur at an expected frequency of once per 274.5 years per person suggested it was unlikely, if extent, to be of epidemiologic importance. Moreover, we identified no improvement in model fit (defined as a lower value of the Akaike Information Criterion) when incorporating ω_N ($\mathrm{AIC}_0 = -46.1$, $\mathrm{AIC}_{\omega_N} = -43.4$).

Modeling cohort-specific susceptibility to mumps under waning vaccine-derived protection

Relating case notification rates to transmission rates

We modified the transmission model described above ('*Model of mumps transmission'*) to capture changes over time in the proportion of individuals susceptible to mumps (*S*), those with immunity acquired through natural infection (*I*), those with protection acquired from vaccination (*V*), and those who have experienced vaccine failure (*F*) due to an unsuccessful initial "take" (primary vaccine failure) or waning of initial protection (secondary vaccine failure). In the US, children have been recommended to receive vaccine doses at age 1 and between ages 4-6 before school entry. We model receipt of each dose in a proportion ($\boldsymbol{\eta}_1$ and $\boldsymbol{\eta}_2$) of individuals as they transition from the 0-11m to 1-4y age classes (first dose) and from the 1-4y to 5-9y age classes

(second dose), assuming those who refuse the first dose do not seek out the second dose either. Defining $\eta_1(i)$=0 for i>1 (corresponding to the 0-11m age group) and $\eta_2(i)$=0 for $i\neq2$ (corresponding to the 1-4y age group),

$$\dot{S}(i,t) = \mu(i) - [\lambda(i,t) + \alpha(i)]S(i,t) + \alpha(i-1)[1-\eta_1(i-1,t)]S(i-1,t)$$

$$\dot{R}(i,t) = \lambda(i,t)[S(i,t) + F(i,t)] - \alpha(i)R(i,t) + \alpha(i-1)R(i-1,t)$$

$$\dot{V}(i,t) = -[\omega_V + \alpha(i)]V(i,t) + \alpha(i-1)(\nu[\eta_1(i-1,t)S(i-1,t) + \eta_2(i-1,t)F(i-1,t)] + V(i-1,t))$$

$$\dot{F}(i,t) = -[\lambda(i,t) + \alpha(i)]F(i,t) + \omega_V V(i,t) + \alpha(i-1)\big((1-\nu)[\eta_1 S(i-1,t) + \eta_2 F(i-1,t)] + (1-\nu\eta_2)F(i-1,t)\big).$$

Numerous studies have shown that 70% (=π_U) of mumps infections cause symptoms in previously susceptible, unvaccinated individuals *(55, 60, 61)*, suggesting ρ/π_U=5.3% of symptomatic infections are reported. Symptoms are estimated to occur in 27.0% to 38.6% of vaccinated individuals, suggesting 44.5% to 61.4% partial protection against symptoms persists even when vaccination fails to prevent infection due to primary or secondary failure *(41)*. As this range was calculated assuming differing serological cutoffs for infection in the absence of a gold standard, we took $\pi_V \sim \text{Unif}(0.270, 0.386)$. Such estimates of vaccine effectiveness against symptoms given infection are consistent with evidence of moderate protection against complications (including endpoints such as orchitis, meningitis, viruria, pancreatitis, and hospitalization) in studies of mumps infections among vaccinated and unvaccinated persons *(62–64)*.

We back-calculated the cumulative force of infection to which individuals in each age group were exposed each year by updating the *S*, *R*, *V*, and *F* classes, thereby relating transmission to case notification data according to the expected proportion of infections causing symptoms and being reported:

$$\Lambda(i,t) = \lambda(i,t)\frac{\rho}{\pi_U}\frac{\pi_U S(i,t) + \pi_V F(i,t)}{N(i,t)},$$

so that

$$\lambda(i,t) = \Lambda(i,t)\frac{\pi_U}{\rho}\frac{N(i,t)}{\pi_U S(i,t) + \pi_V F(i,t)}.$$

We obtained time series of the mean annual force of infection for each of 1,000 draws from the independent distributions of $\{\nu, \widehat{\boldsymbol{Y}}^*\}$ and π_V. As a sensitivity analysis, we repeated the procedure allowing the proportion of infections reported to vary over time (*below, 'Sensitivity analysis under time-varying reporting'*).

In addition to providing estimates of the population susceptible to mumps each year since vaccine rollout, this approach allowed us to assess changes over time in transmission rates that

may result from changes in demography and contact patterns, behavior, health status, and response efforts aiming to limit transmission. We quantify changes in the rate of mumps acquisition per infectious exposure over time as

$$\delta(i,t) = \frac{\lambda(i,t)}{\beta(i)\sum_{j=1}^{10} C_{(S)}(i,j)\frac{I(j,t)}{N(j,t)}},$$

obtaining estimates of $R_0(t)$ as the maximum eigenvalues of the matrix composed of elements

$$\delta(i,t)\frac{\beta(i)C_{(S)}(i,j)N(i)}{\gamma N(j)}.$$

Declining values of $R_0(t)$ over time from 4.79 in the pre-vaccination era to 2.41 (1.85-3.38) as of 2016 indicate that reductions in mumps incidence after vaccine licensure have been attributable to changes in transmission dynamics beyond individual and herd protection conferred by the vaccine (**fig. S2**). This finding persisted in models assuming annual reductions in reporting (*below, 'Sensitivity analysis under time-varying reporting'*).

Our inference of reduced transmission potential during the second half of the twentieth century is consistent with declines in the burden of other pediatric infectious diseases including pneumonia *(65)*, rotavirus diarrhea *(66)*, and central nervous system infections *(67)* preceding licensure of vaccines against the causative agents (*Streptococcus pneumoniae*, rotavirus, and *Haemophilus influenzae* serotype B and varicella, respectively). Many factors might contribute to these overall reductions in pediatric infectious disease burden. These changes correlate with the prevention of measles-induced immune suppression through widespread measles vaccination *(68)*; with improvements in nutrition and health status suggested by declining prevalence of underweight and anemia in childhood *(69, 70)*; and with declining per-capita birth rates that have contributed to changes in the dynamics of measles, pertussis, and other childhood diseases in tandem with vaccination over the same period *(71–73)*. In addition, implementing enhanced interventions in response to mumps cases amid vaccine rollout could be a factor in reduced transmission potential. Whereas mumps infections were once routine for children, outbreaks in the decades following vaccine licensure have prompted epidemiologic investigations and containment measures including active surveillance and isolation of cases *(31, 32, 74, 75)*. Evidence that vaccinated and unvaccinated persons who acquire infection have equal viral loads in saliva and urine suggests that diminished capacity of vaccinated, infected persons to transmit is not a factor in the observed decline in transmission per infected person *(63)*.

To accompany our analysis of changes in age-specific incidence and susceptibility, we also plotted changes in cohort-specific incidence over time (**fig. S3**). We determined the distribution of birth years among annual reported cases by defining annual incidence as binomially distributed within age groups, with *n* equal to the population of each age and *p* the cases per capita per year; we pooled these distributions to calculate the median and interquartile range of birth years among reported cases. Our outcomes illustrate that cases reported during the outbreaks occurring in the late 1980s and early 1990s arose mostly among individuals recommended to receive one vaccine dose, who were exposed to reduced rates of mumps

transmission in childhood compared to earlier cohorts. Rather than reflecting a continuation of cases within this under-immunized cohort, the resurgence of mumps from 2006 to the present has predominantly affected individuals recommended to receive two vaccine doses, consistent with reports from outbreak investigations *(31, 47, 48, 54)*.

Sensitivity analysis under time-varying reporting

We assessed whether inferred degrees of protection and changes in transmission dynamics could be subject to bias resulting from lower reporting of mumps infections after vaccine rollout (**fig. S4**). Suggested by our finding of lower R_0 values over time, such declines may have arisen in the context of lower public and clinical familiarity with mumps due to reductions in incidence, or if the occurrence of cases outside their historical range of 5-9y impacted detection. We arrived at consistent, declining R_0 estimates over time under differing assumptions about declines in reporting (**fig. S5**).

Interpolating age-specific annual incidence from case notification data

Our analysis uses annual, age-specific incidence rates organized into strata of ages 0-11m, 1-4y, 5-9y, 10-14y, 15-19y, 20-24y, 25-29y, 30-39y, 40-64y, and ≥65y. While these strata were defined based on the usual aggregation of case notifications by the Centers for Disease Control and Prevention *(56)*, aggregations differed by year. When aggregations occurred at smaller (e.g., one year of age) intervals, we calculated the stratum-wide incidence rate as a population-weighted mean across age-specific incidence rates within the stratum. When aggregations crossed age strata (e.g., incidence reported for ages 20-29y, rather than 20-24y and 25-29y), we used linear interpolation to estimate incidence in the stratum of interest based on the ratio of incidence in the stratum of interest to incidence across the aggregated strata in the years immediately preceding and following. For instance, if rates were reported for ages 20-29 in year *t*, we computed incidence at ages 20-24y assuming

$$\frac{\ln Y_t(20 \text{ to } 24)}{\ln Y_t(20 \text{ to } 29)} = \text{mean}\left(\frac{\ln Y_{t-1}(20 \text{ to } 24)}{\ln Y_{t-1}(20 \text{ to } 29)}, \frac{\ln Y_{t+1}(20 \text{ to } 24)}{\ln Y_{t+1}(20 \text{ to } 29)}\right)$$

Overall annual incidence was available from each year, enabling us to use the same linear interpolation approach to estimate age-specific rates when age-specific notifications were aggregated over multi-annual periods (up to 5y long in the data). We illustrate the aggregation of reported data by year and by age group (**fig. S6**) together with estimated age-specific rates. Replication files are available in the github repository referenced in the main text.

Modeling cohort-specific susceptibility to mumps assuming no waning of vaccine-derived protection

As an alternative to the hypothesized role of waning protection, the emergence of mumps virus strains escaping vaccine-derived protection has received attention as a potential explanation for the resurgence of mumps since 2006 *(9, 12)* and reduced vaccine effectiveness in recent outbreaks *(14, 49, 51, 54)*. To provide a basis for simulating transmission dynamics under this scenario (*below, 'Simulating mumps transmission dynamics under vaccine escape'*), we solved

for the force of infection $\lambda(i,t)$, updated the populations of the *S*, *R*, *V*, and *F* states, and estimated changes in transmission $\delta(i,t)$ using the approach described in previously (*'Relating case notification rates to transmission rates'*), this time assuming waning of vaccine-derived immunity was not the explanation for continued transmission (ω_V=0); naturally, longer-lasting vaccine protection leads to higher estimated proportions of individuals protected against vaccine-type (pre-2006) lineages (**fig. S7**). In contrast to our estimates of declining R_0 values over time in the model with waning protection (*' Relating case notification rates to transmission rates'*), we infer that the basic reproductive number would have increased to 8.20 (7.46, 9.09) in order to sustain observed transmission at prevalences of immunity expected in the population without waning of vaccine derived protection.

Simulating mumps re-emergence under situations of waning vaccine-derived protection and vaccine escape

Simulating mumps transmission dynamics under waning vaccine-derived protection

We next sought to understand whether the abrupt resurgence in mumps notifications in the US in 2006 was more consistent with dynamics predicted under a situation of vaccine waning or of vaccine escape. Under the scenario of waning protection, we extend the model presented above ('*Model of mumps transmission*') to include vaccination, as described above ('*Relating case notification rates to transmission rates'*), obtaining the system of equations

$$\dot{S}(i) = \mu(i) - [\lambda(i) + \alpha(i)]S(i) + \alpha(i-1)[1-\eta_1(i-1)]S(i-1)$$

$$\dot{E}(i) = \lambda(i)[S(i) + F(i)] - [\sigma + \alpha(i)]E(i) + \alpha(i-1)E(i-1),$$

$$\dot{I}(i) = \sigma E(i) - [\gamma + \alpha(i)]I(i) + \alpha(i-1)I(i-1),$$

$$\dot{R}(i,t) = \gamma I(i) - \alpha(i)R(i) + \alpha(i-1)R(i-1)$$

$$\dot{V}(i) = -[\omega_V + \alpha(i)]V(i) + \alpha(i-1)(v[\eta_1(i-1)S(i-1) + \eta_2(i-1)F(i-1)] + V(i-1))$$

$$\begin{aligned}\dot{F}(i) = -[\lambda(i) + \alpha(i)]F(i) + \omega_V V(i) \\ + \alpha(i-1)\big((1-v)[\eta_1(i-1)S(i-1) + \eta_2(i-1)F(i-1)] \\ + (1 - v\eta_2(i-1))F(i-1)\big),\end{aligned}$$

where the force of infection

$$\lambda(i) = \delta(i, t = 2006)\beta(i)\sum_{j=1}^{10} C_{(S)}(i,j)\frac{I(j)}{N(j)}.$$

We initialize the model with estimates of the population across *S*, *R*, *V*, and *F* states as of 2006, assuming introductions at randomly-drawn frequencies below expected endemic prevalence. We simulate dynamics in a hypothetical population of 1 million for one year using the Gillespie

(stochastic simulation) algorithm, assuming exponentially-distributed event times *(76)*. We assume infections among susceptible persons are detected with probability ρ, while infections among vaccinated persons are detected with probability $\rho\pi_V/\pi_U$ due to partial protection against symptoms.

Simulating mumps transmission dynamics under vaccine escape

We modified the model to assess the potential transmission dynamics of a mumps virus strain with a partial ability to escape vaccine-derived immune protection. Defining φ ($0<\varphi<1$) as the probability for the introduced strain to infect an exposed individual protected by vaccine-derived immunity, we modify the differential equations above (*' Simulating mumps transmission dynamics under waning vaccine-derived protection'*) as follows:

$$\dot{E}(i) = \lambda(i)[S(i) + F(i) + \varphi V(i)] - [\sigma + \alpha(i)]E(i) + \alpha(i-1)E(i-1)$$

$$\dot{V}(i) = -[\omega_V + \alpha(i) + \varphi\lambda(i)]V(i) + \alpha(i-1)(\nu[\eta_1(i-1)S(i-1) + \eta_2(i-1)F(i-1)] + V(i-1)).$$

We update the force of infection as

$$\lambda(i) = \delta_{\omega_V=0}(i, 2006)\beta(i)\sum_{j=1}^{10} C_{(S)}(i,j)\frac{I(j)}{N(j)},$$

for ω_V=0 to capture the assumption that vaccine-derived protection does not wane. We further assume that although vaccinated individuals may be at risk for acquiring the escape strain, naturally immune individuals are protected. We arrive at this consideration based on evidence of stronger immune responses following natural infection in comparison to vaccination: average anti-mumps neutralizing antibody titers are approximately 16-fold higher in naturally-infected children compared mumps-vaccinated children *(18)*, consistent with observations in measles *(77, 78)* and rubella *(79)*, among other viral infections of childhood *(37, 80)*. At adequate concentrations, such antibodies are expected to neutralize heterologous strains effectively *(25, 26)*.

Comparing predicted dynamics from stochastic simulations

To determine which scenario was more concordant with observed cases, we compared model-predicted age-specific and overall incidence rates against reported rates, as well as the predicted and reported median age of infection. To obtain the predicted median age of infection, we constructed an *in silico* pseudo-population corresponding to the US age distribution as of 2006 (ages 0, 1, 2, …, 80y) and drew multinomial samples of infection ages according to model-predicted total age-specific incidence over one year, calculating the median at each iteration.

Anticipating third-dose impact

Expected protection across ages

The continued aging of individuals who were exposed to high rates of mumps transmission in childhood prior to the 1980s suggests the US population will, in the future, depend largely on vaccine-derived direct and indirect protection against mumps. We estimated prevalence of age-specific protection attainable under the current vaccine dosing schedule, as well as an extended three-dose schedule, to assess the potential for eliminating transmission through vaccination. Simplifying the model from section '*Relating case notification rates to transmission rates'* to account for protection resulting only from immunization,

$$\dot{S}(i) = \mu(i) - \alpha(i)S(i) + \alpha(i-1)[1-\eta_1(i-1)]S(i-1)$$

$$\dot{V}(i) = -[\omega_V + \alpha(i)]V(i) + \alpha(i-1)(\nu[\eta_1(i-1)S(i-1) + \eta_2(i-1)F(i-1)] + V(i-1))$$

$$\begin{aligned}\dot{F}(i) = &-\alpha(i)F(i) + \omega_V V(i) \\ &+ \alpha(i-1)\big((1-\nu)[\eta_1(i-1)S(i-1) + \eta_2(i-1)F(i-1)] \\ &+ (1-\nu\eta_2(i-1))F(i-1)\big)\end{aligned}$$

under the current approach with doses administered at ages 1y and 5y, approximately. With an added third dose administered between ages 15-19y at a rate $r_3(i)$,

$$\begin{aligned}\dot{V}(i) = &-[\omega_V + \alpha(i)]V(i) + \alpha(i-1)(\nu[\eta_1(i-1)S(i-1) + \eta_2(i-1)F(i-1)] + V(i-1)) \\ &+ r_3(i)F(i)\end{aligned}$$

$$\begin{aligned}\dot{F}(i) = &-[\alpha(i) + r_3(i)F(i)] + \omega_V V(i) \\ &+ \alpha(i-1)\big((1-\nu)[\eta_1 S(i-1) + \eta_2 F(i-1)] + (1-\nu\eta_2)F(i-1)\big).\end{aligned}$$

We also considered scenarios including boosters at 10y and 20y frequencies for individuals ages 20y and older, included in the above equations via the rate $r_3(i)$. We assumed two scenarios for uptake of these added doses. As a pessimistic case, we assumed that third-dose and booster coverage would resemble the 56% coverage of tetanus-diptheria (Td) booster doses in the US adult population *(81)*. To obtain this coverage level in the population level as a whole, we modeled uptake among 62% of individuals who completed the recommended primary series. As an optimistic case, we assumed the probability for second-dose recipients to obtain a third dose (and for individuals to continue receiving subsequent booster doses) would equate the probability for first-dose recipients to obtain a second dose (97%), resulting in 88% overall third-dose coverage.

Evaluating effective reproductive numbers under extended vaccine dosing schedules

To understand the impact of the vaccine schedules under consideration on transmission dynamics, we calculated the effective reproductive number $R_E(t)$ under steady-state distributions of age-specific susceptibility as the maximum eigenvalue of the matrix with entries

$$\delta(i, t = 2016)\left(\frac{\beta(i)C_{(S)}(i,j)N(i)}{\gamma N(j)}\right)\frac{S(i)+F(i)}{N(i)},$$

using estimates of $\delta(i,t)$ as of 2016 to account for changes in transmission rates.

To determine the threshold level of vaccine protection against emerging strains allowing R_E=1, we defined R_E of an emerging strain as the maximum eigenvalue of a matrix with entries

$$\delta(i, t = 2016)\left(\frac{\beta(i)C_{(S)}(i,j)N(i)}{\gamma N(j)}\right)\frac{S(i) + F(i) + \varphi V(i)}{N(i)},$$

and solving for

$$\underset{\varphi}{\operatorname{argmin}}((R_E(\varphi) - 1)^2).$$

Supplementary figures

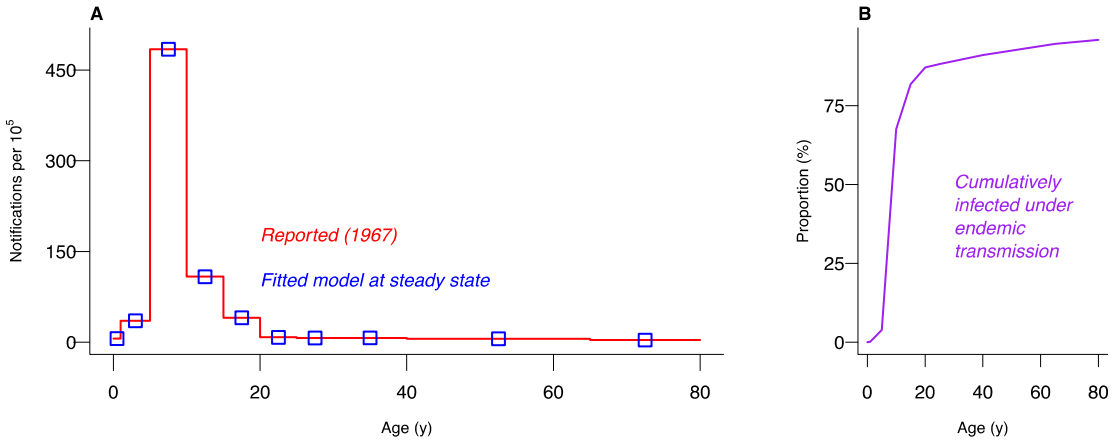

Fig. S1. Fitted endemic transmission dynamics before vaccine rollout. We plot (**A**) reported and model-predicted case notification rates in the years 1960-1964 and (**B**) the corresponding proportion of previously infected and thus immune individuals under estimated transmission rates.

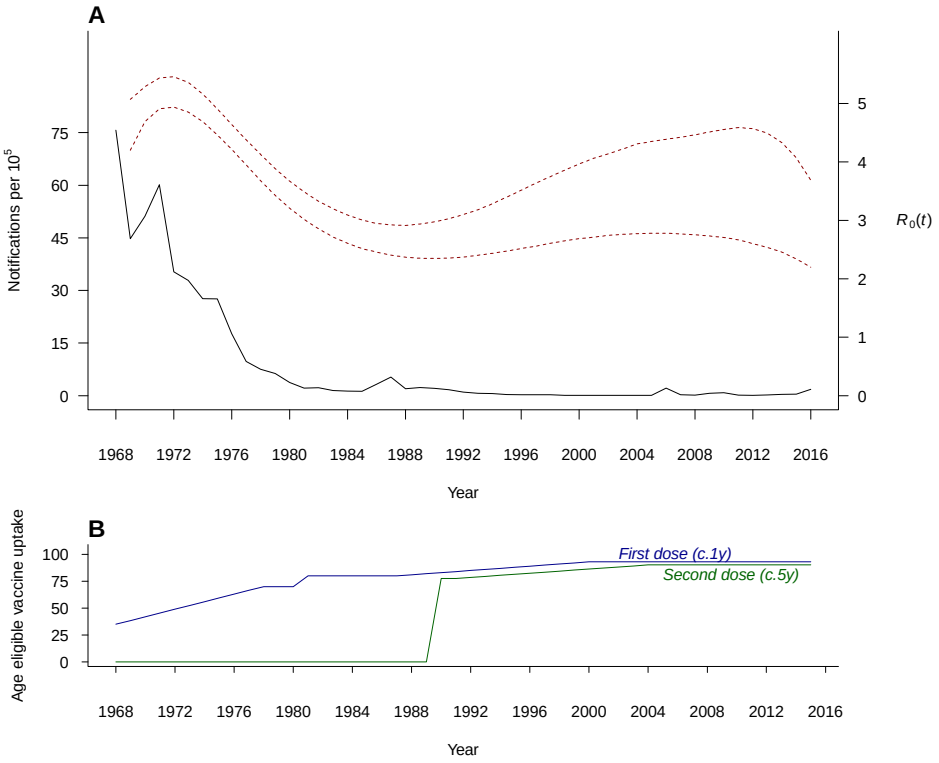

Fig. S2. Reductions in mumps notifications correspond with increases in vaccine coverage and a declining basic reproductive number. We plot (**A**) reported annual incidence rates in the US against our estimates of $R_0(t)$ and (**B**) age-eligible annual vaccine uptake for the first dose (proportion of children receiving at age 1y) and second dose (proportion of children receiving at age 5y), using data from *(2)*. Dotted lines delineate 95% confidence intervals around estimates of $R_0(t)$ as a continuous function of time, fitted individually to evaluations of the conditional distribution of $\delta(i,t)|\{\nu,\omega_V,\pi_V\}$. For each replicate, polynomial terms were added until no improvement was evident in values of the Bayesian Information Criterion.

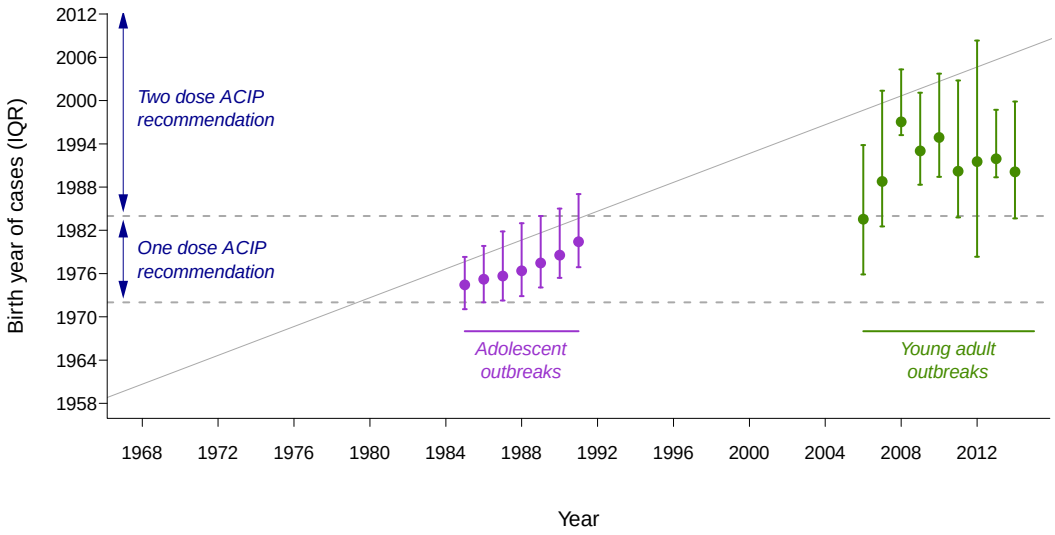

Fig. S3. Birth cohorts accounting for reported cases over time. Illustrating the birth years of reported cases demonstrates that outbreaks following vaccine introduction have affected distinct cohorts. Points and vertical lines indicate medians and interquartile ranges (IQRs) of the birth year of reported cases; the diagonal grey line indicates the expected median age of cases under a continuation of endemic transmission from 1967 forward. Horizontal, dashed lines indicate the birth years associated with one-dose and two-dose vaccination ACIP recommendations, not accounting for state differences in catch-up effort.

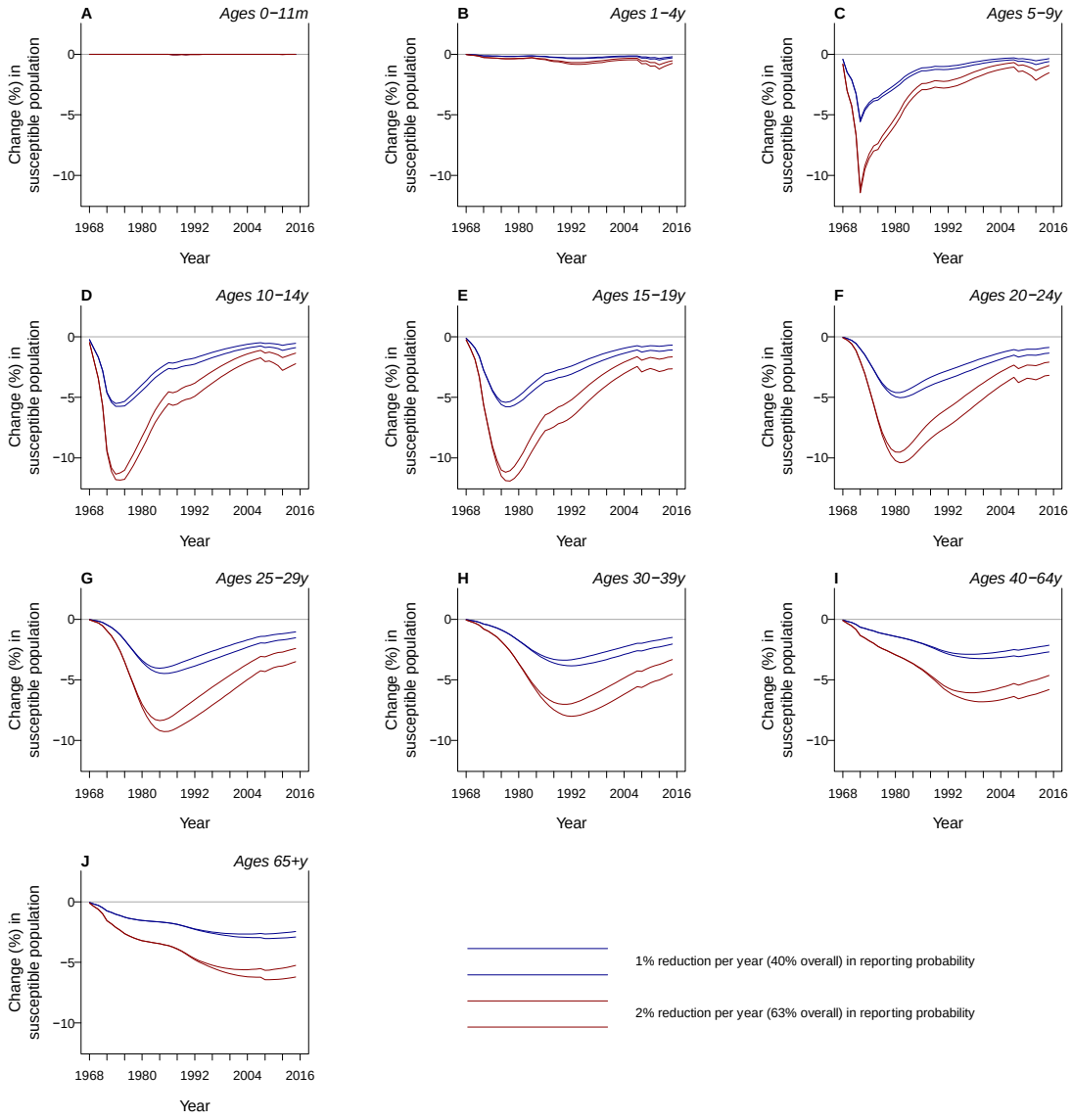

Fig. S4. Changes in estimates of the susceptible population under scenarios of declining reporting. We identify no appreciable changes (>15% departure from original estimate) in age-specific susceptibility when considering 1% and 2% annual reductions in the probability (ρ/π_U) for symptomatic cases to be reported—corresponding to 39% and 63% overall reductions in reporting of symptomatic cases, respectively, between 1967 and 2016 (fig. S4). As an increasing proportion of population immunity has been attributable to mumps vaccination rather than natural mumps infection, the impact of these changes on absolute estimates of the number of people immune to mumps infection declines toward 2016. Shaded areas delineate 95% confidence intervals.

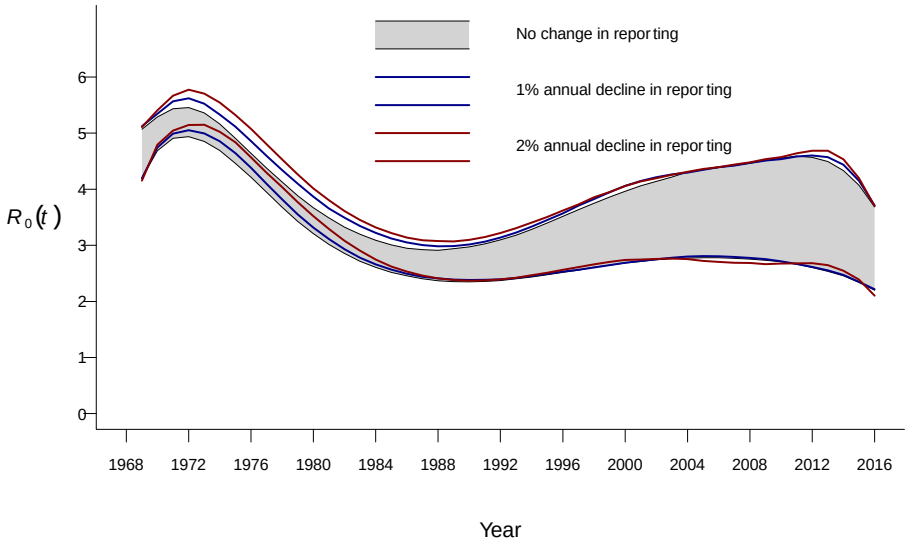

Fig. S5. Changes in estimates of R_0 over time under scenarios of declining reporting. An assumption of declining reporting rates has minimal bearing on estimates of the basic reproductive number. Compared to an original estimate of 2.41 (1.85-3.38) as of 2016 assuming constant reporting, our estimates of 2.43 (1.73-3.28) under 1% annual decreases in reporting and 2.43 (1.74-3.28) under 2% annual decreases demonstrate that this inference is not sensitive to changes in reporting. Shaded areas delineate 95% confidence intervals. Dotted lines delineate 95% confidence intervals around estimates of $R_0(t)$ as a continuous function of time, fitted individually to evaluations of the conditional distribution of $\delta(i,t)|\{\nu,\omega_V,\pi_V\}$. For each replicate, polynomial terms were added until no improvement was evident in values of the Bayesian Information Criterion.

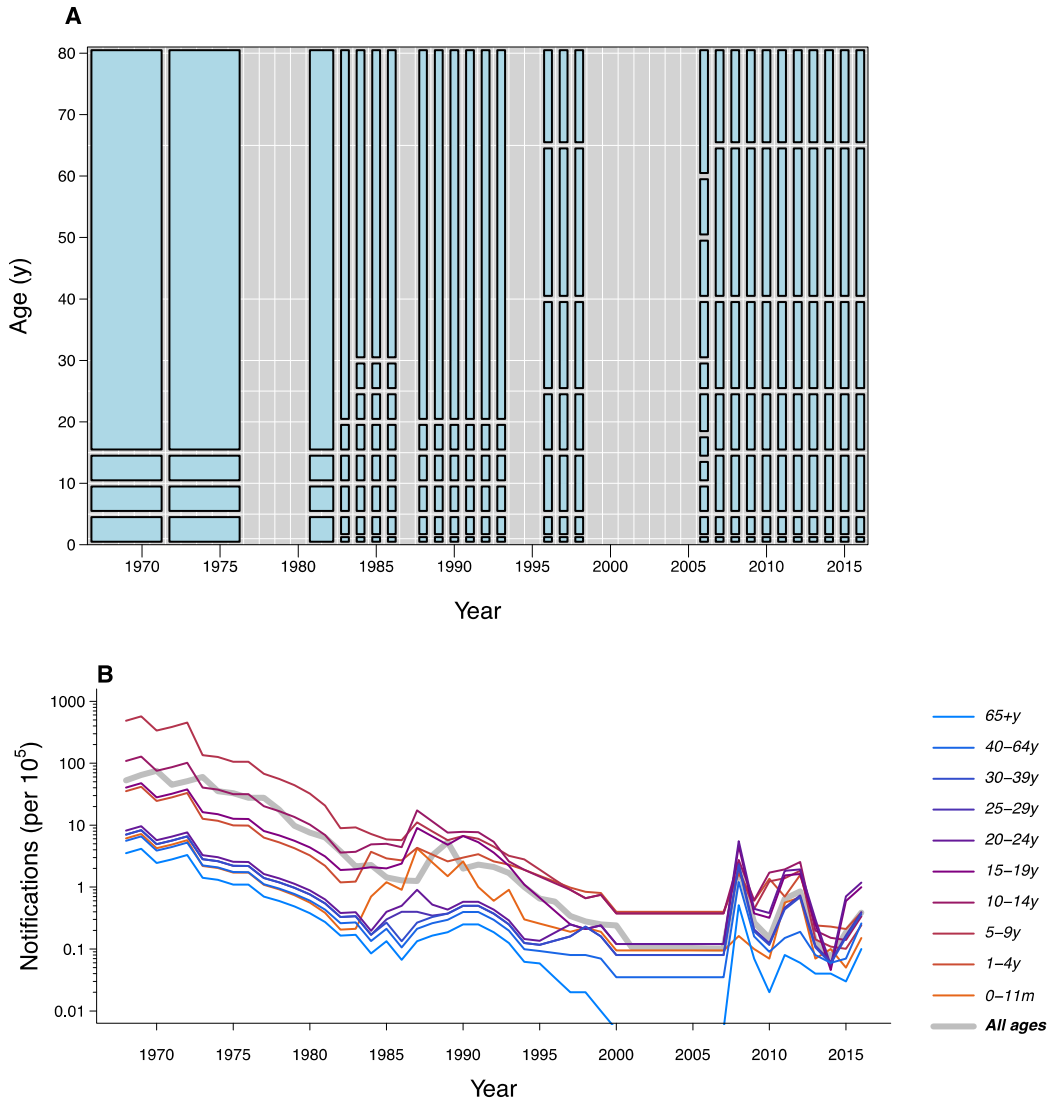

Fig. S6. Aggregated age-specific notification rates. We illustrate the strata at which annual age-specific notification rates were reported as bins (**A**) together with estimated incidence rates by age group (**B**). Reporting of mumps cases was discontinued from 1999 to 2005 *(56)*. We digitized aggregated incidence over this period from Figure 1 in *(2)* assuming constant proportions of cases by age; this assumption had little impact since overall notification rates were low (<1 per 100,000) over this period.

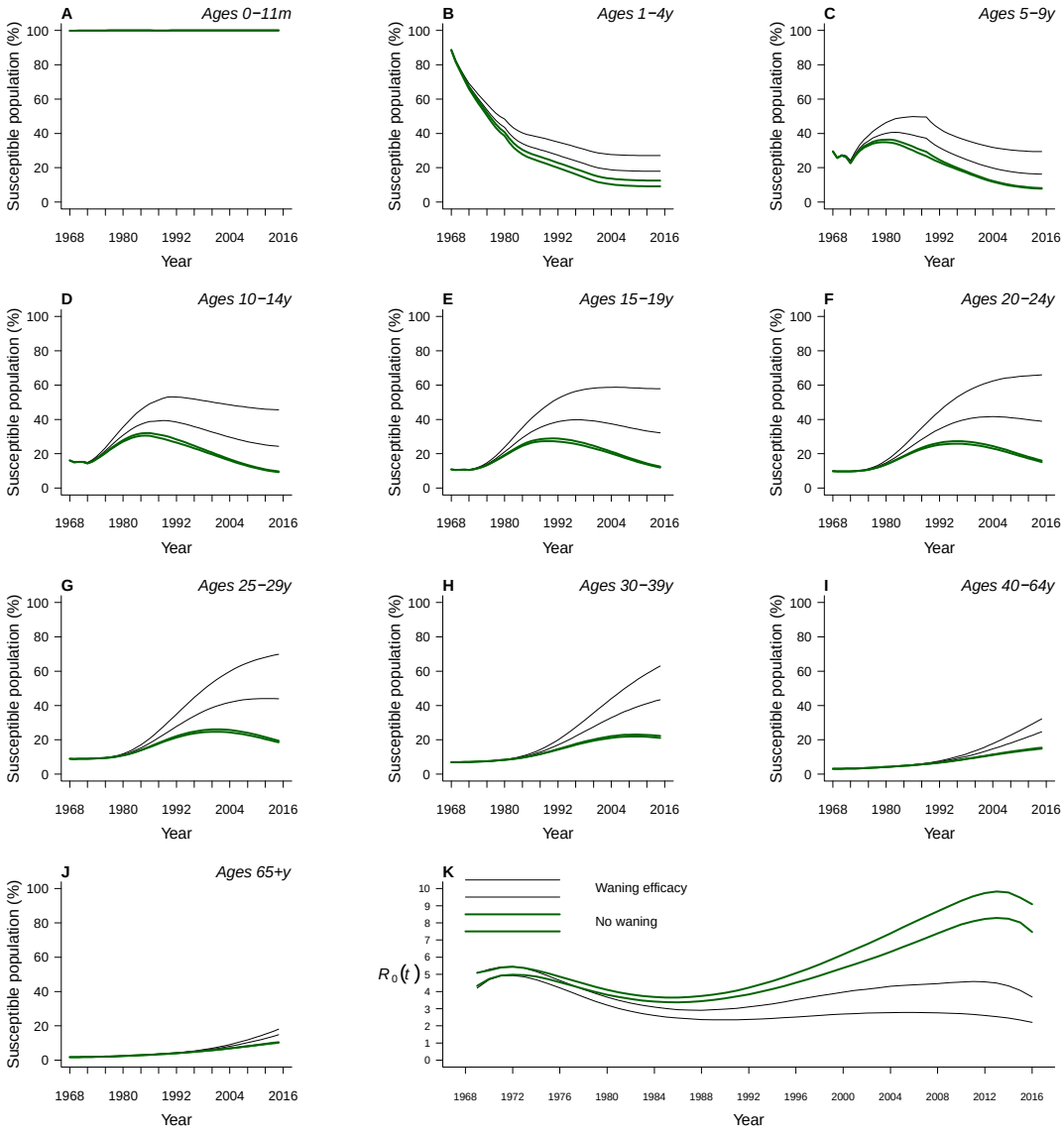

Fig. S7. Estimates of population susceptibility and $R_0(t)$ under an assumption of time-invariant protection. (**A**–**J**) Under the assumption that protection against mumps does not wane with time since vaccination, the susceptible population is estimated to have decreased at ages <15y and to have increased to a lesser extent at older ages. Transient increases in susceptibility at ages 5-9y, 10-14y, 15-19y, and 20-24y reflect reduced incidence and incomplete vaccine uptake during the decades immediately following vaccine rollout. (**K**) We infer that, for transmission to be sustained as reported, R_0 would have increased nearly two-fold to 8.20 (7.46, 9.09) as of 2016. Shaded areas delineate 95% confidence intervals.

Supplementary tables

Table S1. Studies included in meta-analysis assessing vaccine waning. Here we present data from all studies identified in our systematic review and included in the meta-analysis of time-varying vaccine effectiveness (**fig. 1**).

Citation	Ref.	Design	Population	Average time from vaccination to exposure (y)	Doses received	RR (95% CI), ref. 0 doses
Cohen et al., *Emerg Infect Dis* (2007)	*(49)*	Retrospective cohort	Primary and middle school children in the United Kingdom (screening method of *(50)*)	1	1	0.04 (0.01, 0.19)
				4.5	1	0.06 (0.02, 0.16)
				6.5	1	0.1 (0.05, 0.19)
				8.5	1	0.13 (0.07, 0.25)
				10.5	1	0.34 (0.17, 0.7)
				0.5	2	0.01 (0, 0.03)
				2.5	2	0.04 (0.02, 0.07)
				4.5	2	0.08 (0.05, 0.12)
				6.5	2	0.14 (0.07, 0.26)
Vandermeulen et al., *Vaccine* (2004)	*(51)*		Kindergarten and primary school contacts of mumps cases in Belgium	0.5	1 or 2	0.13 (0.04, 0.49)
				1	1 or 2	0.19 (0.07, 0.51)
				2	1 or 2	0.16 (0.06, 0.44)
				3	1 or 2	0.2 (0.08, 0.52)
				4	1 or 2	0.41 (0.21, 0.8)
				5	1 or 2	0.43 (0.22, 0.84)
				6	1 or 2	0.36 (0.17, 0.76)
				7	1 or 2	0.39 (0.19, 0.79)
				8	1 or 2	0.8 (0.46, 1.4)
				9	1 or 2	0.96 (0.54, 1.69)
				10	1 or 2	0.48 (0.13, 1.74)
Hilleman et al., *NEJM* (1967)	*(13)*	Prospective cohort	Classroom contacts of mumps cases in Pennsylvania	0.5	1	0.05 (0.01, 0.18)
		Prospective cohort	Household contacts of mumps cases in Pennsylvania	0.5	1	0.04 (0, 0.56)
Tizes et al., *MMWR* (1973)	*(52)*	Retrospective cohort	Kindergarten and primary school contacts of mumps cases in New York	9.67	1	0.25 (0.13, 0.51)
Schlegel et al., *BMJ* (1999)	*(53)*	Retrospective cohort	Community contacts (ages 5-13) of mumps cases in Switzerland	8	1	0.22 (0.08, 0.59)
Marin et al., *Vaccine* (2008)	*(54)*	Retrospective cohort		0.5	2	0.05 (0, 0.87)
				2.5	2	0.32 (0.1, 1.02)
				4.5	2	0.05 (0, 0.96)
				6.5	2	0.14 (0.04, 0.51)
				8.5	2	0.18 (0.06, 0.54)
				10.5	2	0.25 (0.09, 0.74)
				12.5	2	0.19 (0.07, 0.51)
				14.5	2	0.2 (0.08, 0.54)
				16.5	2	0.33 (0.06, 1.98)
				18.5	2	0.09 (0, 1.56)

Table S2. Model parameter definitions and values. We define parameters included in our ordinary differential equation model together with their values and sources.

Parameter	Definition	Value (95% CI)	Source
ν	Vaccine efficacy at 6 months (proportion of recipients initially protected)	96.4% (94.0-97.8%)	Estimated
$1/\omega_V$	Expected duration of vaccine-derived protection against infection	27.4y (16.7-51.1y)	Estimated
ω_N	Expected duration of naturally-acquired protection against infection	274.5 years (est.); not included in model	Estimated
$\lambda(i)$	Force of infection exerted on individual in the ith age group	Varies (Figure S1)	
$1/\sigma$	Expected duration of incubation period	17d	*(55)*
$1/\gamma$	Expected duration of infectiousness	5d	*(55)*
$1/\mu$	Average life expectancy	80y	N/A
$\alpha(i)$	Rate of aging from the ith group	Inverse of residence time (y) in age group	N/A
$\beta(i)$	Probability of infection in the ith age group per infectious contact		Estimated
i=1		0.024	
i=2		0.127	
i=3		0.125	
i=4		0.175	
i=5		0.079	
i=6		0.050	
i=7		0.035	
i=8		0.088	
i=9		0.148	
i=10		0.004	
$C_{(S)}(i,j)$	Encounter rate between the ith and jth age groups	(varies)	*(57)*
ρ	Proportion of infections reported	3.7%	Estimated
π_U	Probability of clinical symptoms given mumps infection in an unvaccinated individual	70%	*(55)*
π_V	Probability of clinical symptoms given mumps infection in a vaccinated individual susceptible to infection	0.328 (0.273-0.383)	*(41)*
$\Lambda(i)$	Reported rate of age-specific clinical mumps notifications in the ith age group	Varies (Figure 2, Figure S5)	*(56)*
$\eta_1(i)$	Proportion of age-eligible children (1y) receiving first vaccine dose	Varies (Figure S2)	*(2)*
$\eta_2(i)$	Proportion of age-eligible children (2y) receiving first vaccine dose	Varies (Figure S2)	*(2)*
$\delta(i)$	Change in transmission rate to ith age group	Varies (Figure S2, Figure S6)	Estimated
φ	Relative risk of acquiring vaccine-mismatched strain (vs. 1967-type virus) in an individual protected by previous mumps vaccination	0% to 99%	Varied